

The Formation of Massive Stars and Star Clusters

Jonathan C. Tan

Princeton University Observatory, Princeton NJ 08544, USA, and
Dept. of Astronomy, UC Berkeley, CA 94720, USA.

Christopher F. McKee

Depts. of Physics and Astronomy, UC Berkeley, Berkeley, CA 94720,
USA.

Abstract. We model the formation of high-mass stars, specifying the accretion rate in terms of the instantaneous and final mass of the star, the ambient pressure of the star-forming region and the form of polytropic pressure support of the pre-stellar gas core. The high pressures typical of Galactic regions of massive star formation allow a $100 M_{\odot}$ star to form in $\sim 10^5$ yr with a final accretion rate $\sim 10^{-3} M_{\odot} \text{ yr}^{-1}$. By modeling protostellar evolution we predict the properties of several nearby massive protostars. We model cluster formation by applying this theory to many stars. We use the observed intensity of outflows from protoclusters to estimate the star formation rate, finding that clusters take at least several free-fall times to form; for a cluster similar to the Orion Nebula Cluster, we predict a formation timescale $\sim 1 \times 10^6$ yr.

1. Introduction

If there were no massive ($m_* > 8M_{\odot}$) stars, the heavens would appear quite dull. Deprived of many of the heavy elements, it is not clear that Earth-like astronomers could even exist to contemplate the obscurity of such a universe. Fortunately, back in our own cosmos, we can be thankful for the existence of high-mass stars and perhaps devote some effort to understand them and how they come about. All massive stars appear to form in clusters, where they are greatly outnumbered by their lower-mass cousins, and so the questions of how an individual massive star forms and how the cluster forms are intimately entwined.

In this article we first outline a theory for the formation of individual stars, including massive ones, by accretion (§2, taken from McKee & Tan 2002; hereafter MT02). High pressures in the star-forming region result in rapid accretion rates, which allow massive stars to form in spite of the fierce glare of their radiation (Wolfire & Cassinelli 1987), and to do so swiftly before stellar evolution has time to age the newborn stars. In certain regions of the Galaxy, the required high pressures are known to result from the weight of hundreds to thousands of solar masses of strongly self-gravitating and turbulent gas, condensed into *clumps* of order a parsec across. A large fraction of this material inevitably collapses into a stellar cluster, with most of the mass partitioned into relatively low-mass stars.

The massive stars are expected to form preferentially at the center of the clump, where the pressures are highest. We apply our theory for individual star formation to model the birth of the cluster (§§3 & 4, taken from Tan & McKee 2002a; hereafter TM02). Extrapolating models of outflows from low-mass protostars to those from higher masses, we use observations of protocluster outflow intensities to estimate the star formation rates and cluster formation times.

2. Collapse of Turbulent Cloud Cores and Massive Star Formation

Our basic assumption is that a star forms from the gravitational collapse of a molecular cloud *core* that begins in approximate hydrostatic equilibrium; in particular, it does not form by the coalescence of low-mass stars (Bonnell, Bate, & Zinnecker 1998) or by the sweeping up of ambient clump material (Bonnell et al. 1997). On dimensional grounds we then expect that the protostellar accretion rate is given by

$$\dot{m}_* = \phi_* \frac{m_*}{t_{\text{ff}}}, \quad (1)$$

where $t_{\text{ff}} = (3\pi/32G\rho)^{1/2}$ is the free-fall time and ϕ_* is a dimensionless constant of order unity. This equation has the same dependence on dimensional parameters as that for isothermal collapse, $\dot{m}_* \simeq c_{\text{th}}^3/G$ (Shu 1977), if the thermal sound speed, c_{th} , is replaced by the virial velocity $(Gm_*/R)^{1/2}$, since $(Gm_*/R)^{3/2}/G \propto m_*(Gm_*/R^3)^{1/2} \propto m_*/t_{\text{ff}}$. We have shown (MT02) that if the collapse is spherical and self-similar, then ϕ_* is quite close to unity provided that the value of ρ entering t_{ff} is evaluated at the radius in the initial cloud that just encloses the gas that goes into the star when its mass is m_* . We summarize these results below. Collapse to the star will naturally proceed via a disk, where we assume instabilities drive high inflow rates if the disk mass grows to be a significant fraction of the star's (Shu et al. 1990).

First we allow for the disruptive effect of protostellar outflows on the gas core so that only a fraction $\epsilon_{\text{core}} = m_*/M$ of the core mass can accrete onto the star. The value of ϵ_{core} is uncertain for massive stars, since it depends on the unknown properties of their protostellar winds. We assume that it is constant over the accretion history of the star, and for numerical estimates set $\epsilon_{\text{core}} = 0.5$, similar to the value calculated for low-mass stars (Matzner & McKee 2000).

For the core, we assume a spherical power-law ambient medium, which ensures accretion is self-similar. With $\rho \propto r^{-k_\rho}$ and $P \propto r^{-k_P}$, it follows that the core is a polytrope with $P \propto \rho^{\gamma_p}$. In hydrostatic equilibrium (HSE) $k_\rho = 2/(2 - \gamma_p)$ and $k_P = \gamma_p k_\rho = 2\gamma_p/(2 - \gamma_p)$ (McLaughlin & Pudritz 1996). Let $c \equiv (P/\rho)^{1/2}$ be the effective sound speed. The equation of HSE then gives $M = (k_P c^2 r)/G$ and $\rho = A c^2/(2\pi G r^2)$, with $A = \gamma_p(4 - 3\gamma_p)/(2 - \gamma_p)^2$. Equation (1) then implies

$$\dot{m}_* = \phi_* \epsilon_{\text{core}} \frac{4}{\pi\sqrt{3}} k_P A^{1/2} \frac{c^3}{G}, \quad (2)$$

which is a generalization of the isothermal accretion rate to the nonthermal case.

For the polytropic sphere, $\rho \propto r^{-k_\rho}$ and $M \propto r^{3-k_\rho}$, which implies $\rho \propto M^{-k_\rho/(3-k_\rho)} = M^{-2/(4-3\gamma_p)}$. Thus we have $\dot{m}_* \propto m_* \rho^{1/2} \propto m_*^{1-1/(4-3\gamma_p)}$ for the

mass dependence of the accretion rate. Integration yields

$$m_* = m_{*f} \left(\frac{t}{t_{*f}} \right)^{4-3\gamma_p}, \quad (3)$$

where m_{*f} is the final stellar mass, which is attained at a time t_{*f} (McLaughlin & Pudritz 1997, hereafter MP97). Note that for $\gamma_p < 1$ the accretion rate accelerates (MP97). Equation (3) implies

$$\dot{m}_* = (4 - 3\gamma_p) \frac{m_*}{t} = (4 - 3\gamma_p) \frac{m_{*f}}{t_{*f}} \left(\frac{t}{t_{*f}} \right)^{3-3\gamma_p}. \quad (4)$$

As discussed by MP97, termination of the accretion breaks the self-similarity once the expansion wave reaches m_{*f} . This occurs at a time they label t_{ew} , which is about $0.45t_{*f}$. Thereafter, equation (4) becomes approximate, but they argue that the approximation should be reasonably good. From equations (1) and (4), the star-formation time is

$$t_{*f} = \frac{(4 - 3\gamma_p)}{\phi_*} t_{\text{ff}}. \quad (5)$$

Using the results of MP97, we can evaluate ϕ_* in the non-magnetic case,

$$\phi_{*\text{non}} = (4 - 3\gamma_p) \frac{t_{\text{ff}}}{t_{*f}} = \pi\sqrt{3} \left[\frac{(2 - \gamma_p)^2 (4 - 3\gamma_p)^{(7-6\gamma_p)/2} m_0}{8^{(5-3\gamma_p)/2}} \right]^{1/(4-3\gamma_p)}, \quad (6)$$

where m_0 is tabulated by MP97. For example, for the singular isothermal sphere the parameter $m_0 = 0.975$ and $\phi_{*\text{non}} = 0.975\pi\sqrt{3}/8 = 0.663$. For other values of γ_p in the range $0 \leq \gamma_p \leq 1$, $\phi_{*\text{non}} \simeq 1.13/(1 + 0.7\gamma_p^2)$. We conclude that $\dot{m}_* \simeq m_*/t_{\text{ff}}$ to within a factor 1.5 for spherical cores in which the effective sound speed increases outward.

We can estimate the effect of magnetic fields on the accretion rate from the work of Li & Shu (1997), who considered collapse of self-similar, isothermal, magnetized, toroidal clouds. The equilibrium surface density is $\Sigma = (1 + H_0)c_{\text{th}}^2/(\pi G\varpi)$, where ϖ is the cylindrical radius and H_0 is a parameter that increases from zero as the magnetic field is increased. They show that the accretion rate is $\dot{m}_* = 1.05(1 + H_0)c_{\text{th}}^3/G$, which is larger than the isothermal case by about a factor $(1 + H_0)$. However, equation (1) predicts $\dot{m}_* \propto M\rho^{1/2} \propto M^{3/2}/\varpi^{3/2} \propto \Sigma^{3/2}\varpi^{3/2} \propto (1 + H_0)^{3/2}$. To reconcile this result with the correct value, we require $\phi_* \simeq \phi_{*\text{non}}/(1 + H_0)^{1/2}$. They regard $H_0 \sim 1$ as typical for low-mass star formation, which would lead to a reduction in the accretion rate (as expressed in eqs. [1] and [2]) by a factor of about 1.4.

The power-law structure of cloud cores is truncated by the ambient pressure in the star-forming clump, which is thus equivalent to the core surface pressure, P_s . We parameterize the rate of individual core collapse in terms of this pressure, which we then relate to the clump's surface density. A higher ambient pressure means that a core of a given mass is truncated at higher density and thus its free-fall and star formation timescales are shorter.

Since $\rho_s = P_s/c_s^2$, $M = (k_P c^2 r)/G$ and $\rho = A c^2/(2\pi G r^2)$, the density at the surface of the core is

$$\rho_s = \left(\frac{A k_P^2 \epsilon_{\text{core}}^2 P_s^3}{2\pi G^3 m_{*f}^2} \right)^{1/4}. \quad (7)$$

The general expression for the accretion rate in terms of the surface pressure and the final stellar mass can now be inferred from equations (1) and (7):

$$\dot{m}_* = 4.02 \times 10^{-4} \phi_* (A k_P^2 \epsilon_{\text{core}}^2)^{1/8} \left(\frac{m_{*f}}{30 M_\odot} \right)^{3/4} \left(\frac{P_s}{10^8 \text{ K cm}^{-3}} \right)^{3/8} \left(\frac{m_*}{m_{*f}} \right)^{\frac{3(2-k_\rho)}{2(3-k_\rho)}} M_\odot \text{ yr}^{-1} \quad (8)$$

and the corresponding value of the star-formation time is

$$t_{*f} = 7.47 \times 10^4 \left(\frac{4 - 3\gamma_p}{\phi_* A^{1/8} k_P^{1/4} \epsilon_{\text{core}}^{1/4}} \right) \left(\frac{m_{*f}}{30 M_\odot} \right)^{1/4} \left(\frac{10^8 \text{ K cm}^{-3}}{P_s} \right)^{3/8} \text{ yr}. \quad (9)$$

The accretion rate and star formation time depend to some extent on the value of k_ρ in the protostellar cores. No data are available on the structure of cores that are forming very massive stars. For “high-mass” cores in Orion, Caselli & Myers (1995) find $k_\rho \simeq 1.45$ with a dispersion of ± 0.2 . According to van der Tak et al. (2000), the clumps in which high-mass cores are embedded have values of k_ρ ranging from 1 to 2, centered around 1.5. For numerical evaluation of the accretion rate, we shall adopt $k_\rho = 1.5$, which corresponds to $\gamma_p = 2/3$, $k_P = 1$, $A = 3/4$, and $\phi_{*\text{non}} = 0.90$. In this case, the protostellar accretion rate varies linearly with time, $\dot{m}_* \propto t$. So long as $A \propto \gamma_p = 2(k_\rho - 1)/k_\rho$ is not near zero, the star-formation time is relatively insensitive to k_ρ . For $k_\rho = 1.5$, the numerical coefficient in equation (8) is $3.49 \times 10^{-4}/(1 + H_0)^{1/2} M_\odot \text{ yr}^{-1}$ and $\dot{m}_* \propto (m_*/m_{*f})^{0.5}$. Similarly, the numerical coefficient in equation (9) becomes $1.72 \times 10^5 (1 + H_0)^{1/2} \text{ yr}$.

At present, direct observations of the total pressure at the surface of a core that will form a massive star are not available, so we must estimate this pressure theoretically. Since the core is embedded in a turbulent clump, its pressure will fluctuate, but the time-averaged surface pressure for the typical core should be approximately the same as the spatial average of the pressure in the clump, $P_s = \phi_P \bar{P}$, where ϕ_P is a parameter of order unity. The mean pressure in a clump is (MT02):

$$\bar{P} = \left(\frac{3\pi f_{\text{gas}} \phi_B \alpha_{\text{vir}}}{20} \right) G \Sigma^2, \quad (10)$$

where f_{gas} is the fraction of the clump mass in gas (as opposed to stars), $\alpha_{\text{vir}} \equiv 5 \langle \sigma^2 \rangle R_{\text{cl}} / G M_{\text{cl}} \equiv M_{\text{vir}} / M_{\text{cl}}$ is the virial parameter, σ is the one-dimensional velocity dispersion, $\langle x \rangle$ indicates a mass-averaged quantity, $\phi_B = \langle c^2 \rangle / \langle \sigma^2 \rangle \simeq 1.3 + 1.5/m_A^2$ represents the contribution of the magnetic pressure, m_A is an average of the Alfvén Mach number, and $\Sigma = M_{\text{cl}}/(\pi R_{\text{cl}}^2)$ is the surface density of the clump, including the mass of any embedded stars. In terms of Σ_{vir} , the surface density determined from the virial theorem, we have $\Sigma = \Sigma_{\text{vir}}/\alpha_{\text{vir}}$.

Regions of high-mass star formation studied by Plume et al. (1997, hereafter P97) are characterized by virial masses $M_{\text{vir}} \sim 3800 M_{\odot}$ and radii ~ 0.5 pc. The corresponding mean column density is $\Sigma_{\text{vir}} \simeq 1 \text{ g cm}^{-2}$; the corresponding visual extinction is $A_V = (N_{\text{H}}/2 \times 10^{21} \text{ cm}^{-2}) \text{ mag} = (\Sigma_{\text{vir}} \times 214) \text{ mag}$. These column densities are far greater than those of giant molecular clouds (GMCs) (0.035 g cm^{-2} —Solomon et al. 1987) or of regions of low-mass star formation (the average Σ in the C^{18}O cores in Taurus is 0.032 g cm^{-2} —Onishi et al. 1996). On the other hand, the central stellar surface density in the Orion Nebula Cluster is about 1 g cm^{-2} (Hillenbrand & Hartmann 1999). The mean density in the Plume et al. clumps is $n_{\text{H}} \simeq 2 \times 10^5 \text{ cm}^{-3}$. As discussed by MT02, the virial parameter $\alpha_{\text{vir}} \simeq 1.3 - 1.4$ for GMCs, whereas it is quite close to unity for cores that are actively forming stars. Although there is no direct determination of α_{vir} for massive star-forming clumps, P97 regard the virial mass as the most accurate, and we adopt $\alpha_{\text{vir}} = 1$ for our numerical estimates.

MT02 discuss the estimates for the other parameters, $\phi_B \simeq 2.8$, $f_{\text{gas}} \simeq 2/3$ and $\phi_P \simeq 2$ needed to determine P_s . Thus from equation (10)

$$P_s = 2.28 \times 10^8 (f_{\text{gas}} \phi_P \phi_B \alpha_{\text{vir}}) \Sigma^2 \text{ K cm}^{-3} \rightarrow 8.5 \times 10^8 \Sigma^2 \text{ K cm}^{-3}. \quad (11)$$

With $\epsilon_{\text{core}} = 0.5$ and $H_0 = 1$, the corresponding protostellar accretion rate is

$$\begin{aligned} \dot{m}_* &= 4.75 \times 10^{-4} \epsilon_{\text{core}}^{1/4} \frac{(f_{\text{gas}} \phi_P \alpha_{\text{vir}} \phi_B)^{3/8}}{(1 + H_0)^{1/2}} \left(\frac{m_{*f}}{30 M_{\odot}} \right)^{3/4} \Sigma^{3/4} \left(\frac{m_*}{m_{*f}} \right)^{0.5} M_{\odot} \text{ yr}^{-1} \\ &\rightarrow 4.6 \times 10^{-4} \left(\frac{m_{*f}}{30 M_{\odot}} \right)^{3/4} \Sigma^{3/4} \left(\frac{m_*}{m_{*f}} \right)^{0.5} M_{\odot} \text{ yr}^{-1}, \end{aligned} \quad (12)$$

and the star formation time is

$$t_{*f} = \frac{1.26 \times 10^5}{\epsilon_{\text{core}}^{1/4} (f_{\text{gas}} \phi_P \alpha_{\text{vir}})^{3/8}} \left[\frac{(1 + H_0)^{1/2}}{\phi_B^{3/8}} \right] \left(\frac{m_{*f}}{30 M_{\odot}} \right)^{1/4} \Sigma^{-3/4} \text{ yr} \quad (13)$$

$$\rightarrow 1.29 \times 10^5 \left(\frac{m_{*f}}{30 M_{\odot}} \right)^{1/4} \Sigma^{-3/4} \text{ yr}. \quad (14)$$

For example, with the fiducial values of our parameters, a $100 M_{\odot}$ star forming in a clump with $\Sigma = 1 \text{ g cm}^{-2}$ has a final accretion rate of $1.1 \times 10^{-3} M_{\odot} \text{ yr}^{-1}$ and a star-formation time of $1.75 \times 10^5 \text{ yr}$. Our result for the accretion rate is somewhat lower than that of Osorio et al. (1999), who found accretion rates by matching the infrared spectra of embedded protostars. Our result for the star formation time is comparable to that of Behrend & Maeder (2001), who performed an analysis based on protostellar outflows, although our result for the time evolution of the accretion rate is quite different.

The above solutions apply to purely nonthermal cores. We have also allowed for an additional thermal ($T \simeq 100 \text{ K}$) component of pressure support (MT02). For typical high pressure star-forming regions cores with $M \gtrsim 1 M_{\odot}$ are dominated by the nonthermal component. This implies that cores are supersonically turbulent and therefore clumpy, which means we expect the accretion rate to exhibit large fluctuations about the mean value. Radiation pressure can reduce the accretion flow to the most massive stars from the values predicted above (Wolfire & Cassinelli 1987; Jijina & Adams 1996; Tan & McKee 2002b).

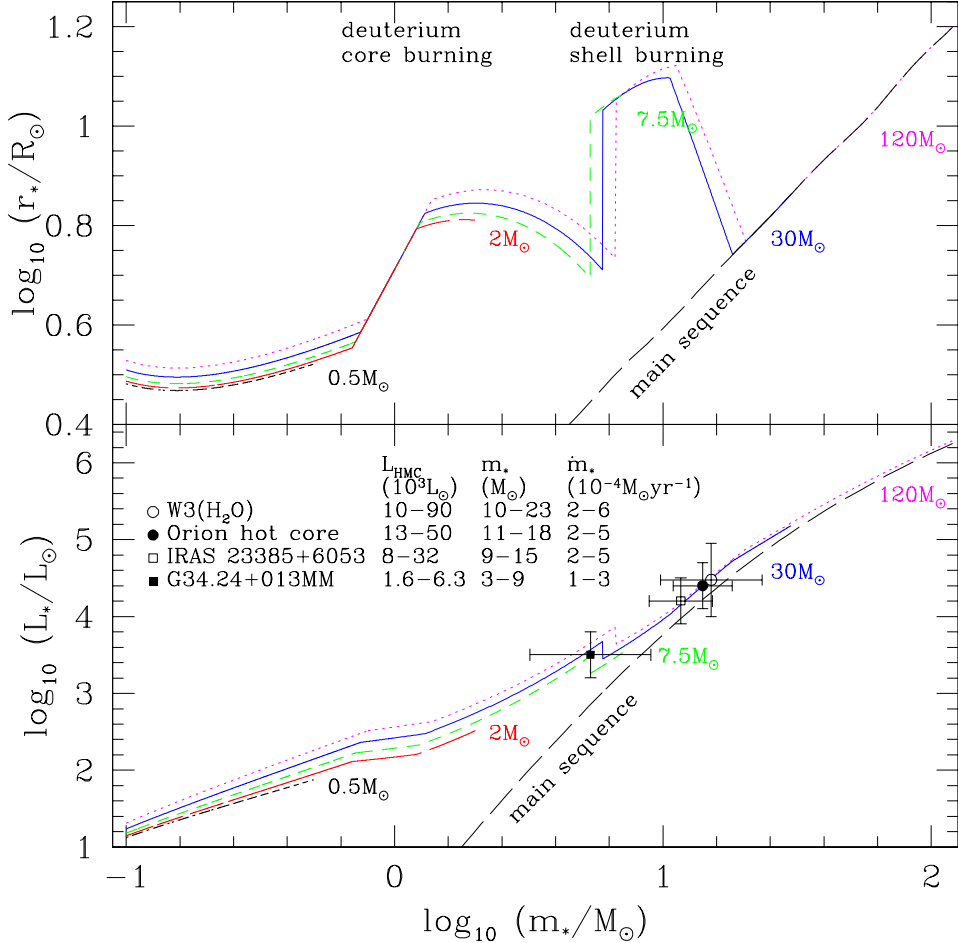


Figure 1. Evolution of protostellar r_* and L_* in a $\Sigma = 1 \text{ g cm}^{-2}$ clump. For references on HMC luminosities see MT02.

3. Protostellar Evolution, Luminosities and Outflows

The properties of accreting protostars depend on their accretion rates (e.g., Stahler, Shu & Taam 1980; Stahler 1988; Palla & Stahler 1992; Nakano et al. 2000). In particular, the accretion luminosity $L_{\text{acc}} = f_{\text{acc}} G m_* \dot{m}_* / r_*$, where f_{acc} is a factor of order unity accounting for energy radiated by an accretion disk or used to drive protostellar outflows, and the stellar radius r_* may depend sensitively on \dot{m}_* . Massive stars join the main sequence during their accretion phase at a mass that also depends on the accretion rate (Palla & Stahler 1992). The intensity of protostellar outflows, at least from low-mass stars, is thought to depend on the accretion rate and the Keplerian velocity, v_K , at the stellar surface (e.g. Shu et al. 1994). To predict protostellar properties and thus compare theory with observation, we require a model of protostellar evolution.

As previous investigations have mostly considered constant accretion rates, we have developed a simple model for protostellar evolution based on that of Nakano et al. (2000), which allows easy implementation of time dependent accretion. The model accounts for the total energy of the protostar as it accretes and dissociates matter, expands and contracts, and, if the central temperature $T_c \gtrsim 10^6$ K, burns deuterium. We have modified Nakano et al.'s model to include additional processes, such as deuterium shell burning, and calibrated these modifications against the more detailed calculations of Stahler (1988) and Palla & Stahler (1992). Protostellar evolution is followed from $m_* = 0.1 M_\odot$ to the end of accretion ($m_* = m_{*f}$). Massive protostars reach the main sequence (Schaller et al. 1992) before they have finished accreting. The evolution of protostellar radius as a star grows in mass is shown in Figure 1 for several different final stellar masses, all forming in a clump with $\Sigma = 1 \text{ g cm}^{-2}$ and $T = 100$ K. Also shown is the evolution in bolometric luminosities (including the contribution from an accretion disk), and our use of these models to predict the masses and accretion rates of protostars thought to be illuminating several nearby hot molecular cores (HMCs). MT02 consider the effect of varying k_ρ and Σ on these estimates and also compare results with Osorio et al. (1999), who have modeled the same sources.

Powerful outflows are ubiquitous from regions of both low and high-mass star formation (e.g., Richer et al. 2000). Models of magnetically driven outflows from a disk (Blandford & Payne 1982) and from the inner edge of a disk (Shu et al. 1994) have been presented. A common feature of these models is the production of a bipolar outflow with momentum distribution $p_w \propto (\sin \theta)^{-2}$ for $\theta > \theta_0$, where θ is measured from the outflow axis and $\theta_0 \sim 10^{-2}$ (Matzner & McKee 1999). On scales large compared to the source (Matzner & McKee 1999)

$$\frac{d\dot{p}_w}{d\Omega} = \frac{\dot{p}_w}{4\pi \ln(2/\theta_0)(1 + \theta_0^2 - \cos^2\theta)}. \quad (15)$$

We parameterize the total momentum flux escaping in the outflow via

$$\dot{p}_w = f_{w,\text{esc}} \dot{m}_w v_w = f_{w,\text{esc}} f_w \dot{m}_* v_w = \phi_w \dot{m}_* v_K, \quad (16)$$

where $f_{w,\text{esc}}$ is the fraction of outflow momentum that escapes from the core, $f_w = \dot{m}_w/\dot{m}_*$, $\phi_w = f_{w,\text{esc}} f_w v_w/v_K$ and v_K is the Keplerian velocity at the equatorial radius of the star. Najita & Shu (1994) considered the acceleration of winds from an accreting $0.5 M_\odot$ protostar. For several different X-wind model boundary conditions their results gave quite a large variation in $f_w \approx 0.1 - 0.8$, but only a small spread in $f_w v_w/v_K \simeq 0.6$ within $\sim 30\%$. Najita & Shu (1994) also showed that v_w is approximately independent of θ so that \dot{m}_w has the same distribution as \dot{p}_w , and thus $f_{w,\text{esc}}$ applies to wind mass as well as momentum. If all the protostellar wind material escapes in two cones of solid angle $\Omega_{w,\text{esc}}$ (opening angle $\theta_{w,\text{esc}}$), and if core material originally inside these cones is also swept up, then

$$\epsilon_{\text{core}} = \frac{1 - 2\Omega_{w,\text{esc}}/(4\pi)}{1 + f_{w,\text{esc}} f_w}. \quad (17)$$

For $\epsilon_{\text{core}} = 0.5$ (Matzner & McKee 2000) and $f_w = 0.1, 0.3, 0.8$ we solve equations (15) (with $\dot{p}_w \rightarrow \dot{m}_w$) and (17) for $f_{w,\text{esc}}$ and $\theta_{w,\text{esc}}$. We find $f_{w,\text{esc}} =$

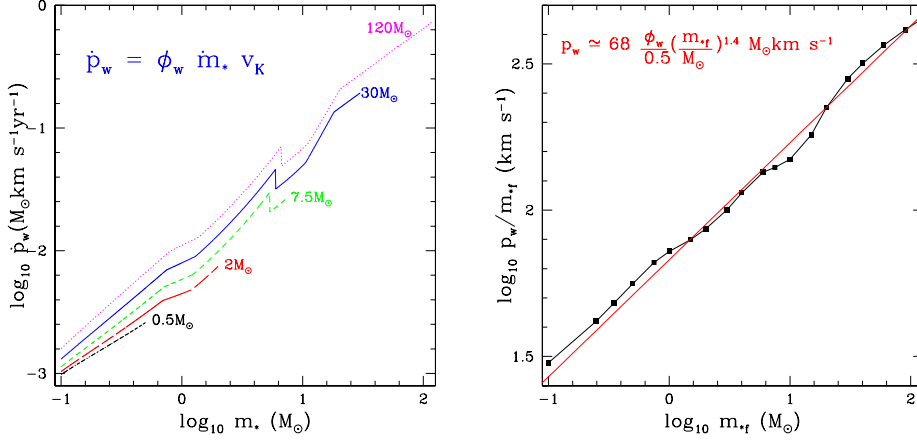


Figure 2. Protostellar outflows. (a) Left: $\dot{p}_w(m_*)$ (b) Right: $p_w(m_{*f})$

0.89, 0.86, 0.79 and $\theta_{w,\text{esc}} = 57^\circ, 51^\circ, 36^\circ$, respectively. The escape efficiencies are quite high because of the concentration of the wind near the outflow axis (eq. [15]). Assuming the wind is atomic, the swept-up gas is molecular and they escape together in a momentum conserving shell, the fraction of momentum leaving the core that is atomic in these three cases is 0.49, 0.62, 0.78, respectively.

We adopt $f_w = 0.3$ and $f_{w,\text{esc}} = 0.86$ as our fiducial values so that $\phi_w \simeq 0.5$, since $f_w v_w / v_K \simeq 0.6$ (Najita & Shu 1994). This estimate is broadly consistent with observations of outflows from low-mass stars (Bontemps et al. 1996). We apply the above model for low-mass protostellar outflows to stars of all masses as they accrete. This application is uncertain: for the X-wind model (Shu et al. 1988) to apply, the stellar surface field strength required by a $10 M_\odot$ protostar with radius $10 R_\odot$ accreting at a few $\times 10^{-4} M_\odot \text{ yr}^{-1}$ is $\sim 10^3 \text{ G}$. The momentum injection rates and total momenta from protostars forming in a $\Sigma = 1 \text{ g cm}^{-2}$ environment are shown in Figure 2. A fit to these results is

$$p_w \approx p_1 m_{*f}^{\alpha_p} = 68 \left(\frac{\phi_w}{0.5}\right) \left(\frac{m_{*f}}{M_\odot}\right)^{1.4} M_\odot \text{ km s}^{-1}. \quad (18)$$

This relation depends only weakly on Σ (TM02).

4. Probing the Rate of Star Formation in Clusters with Outflows

We model the formation of star clusters with $\mathcal{N}_{*f} = M_{*f} / \bar{m}_{*f}$ stars, where M_{*f} is the total stellar mass and \bar{m}_{*f} is the mean individual stellar mass. Stars are drawn from a power-law initial mass function (IMF) truncated above m_{*u} and below m_{*l} and of the form $dF/d \ln m_* = A_* m_*^{-\alpha_*}$, where F is the fraction of all stars that have a mass greater than m_* . The Salpeter (1955) IMF has $\alpha_* = 1.35$, $A_* = 0.0603$ and $\bar{m}_* = 0.353 M_\odot$ for $m_{*l} = 0.1 M_\odot$ and $m_{*u} = 120 M_\odot$. We adopt this as our fiducial IMF. While observational determinations of the IMF indicate deviations from this simple power-law form at lower masses, these have

little effect on most of the feedback processes operating in a protocluster, which are controlled by the massive stars. The total protostellar wind momentum, $p_{w,\text{tot}}$, from the forming star cluster does receive important, approximately equal, contributions from all decades of the IMF, since $\alpha_* \simeq \alpha_p$. However, even in this case, the variation caused by uncertainties in the low-mass IMF is minor. The low-mass stars do dominate the total stellar mass, and this may be parameterized via μ_h , the total stellar mass per high-mass ($m_* > 8 M_\odot$) star, most of which end their life in a core-collapse supernova explosion. For our adopted IMF, $\mu_h = 134 M_\odot$, which is close to the value for the Miller & Scalo (1979) IMF.

We use Monte Carlo simulations to find the median values of the post-accretion luminosity, L_{*f} , and total protostellar outflow momentum released during formation of a cluster of mass M_{*f} . Typical lower-mass clusters fail to fully sample the IMF. For $M_{*f}/M_\odot \gtrsim 1600$, $L_{*f}/M_{*f} \simeq 630 L_\odot M_\odot^{-1}$, while for $100 \lesssim M_{*f}/M_\odot \lesssim 1600$, $L_{*f}/M_{*f} \simeq 436(M_{*f}/1000M_\odot)^{0.8} L_\odot M_\odot^{-1}$. For the outflows, with the fiducial values of the parameters $\Sigma = 1 \text{ g cm}^{-2}$, $T = 100 \text{ K}$, $k_\rho = 1.5$ and $\phi_w = 0.5$, we find

$$\frac{p_{w,\text{tot}}}{M_{*f}} \simeq 87 \left(\frac{\phi_w}{0.5} \right) \left(\frac{M_{*f}}{1000 M_\odot} \right)^{0.14} \text{ km s}^{-1} \quad (M_{*f} < 1000 M_\odot). \quad (19)$$

For $M_{*f} > 1000 M_\odot$, $p_{w,\text{tot}}/M_{*f} \simeq 87(\phi_w/0.5) \text{ km s}^{-1}$. The loss of momentum in outflow-outflow interactions would lower these estimates. However, because of the collimation of momentum in jets (eq.[15]), we expect this effect to be relatively minor, particularly for smaller clusters with fewer simultaneous independent outflows.

Unless triggered by an external influence such as a supernova blast wave, the overall rate at which stars form within a clump is not expected to exceed $\sim M_{*f}/\bar{t}_{\text{ff}}$, where $\bar{t}_{\text{ff}} = (3\pi/32G\bar{\rho})^{1/2}$ is the free-fall time of the clump evaluated at the mean density (stars + gas) at a typical stage in the evolution (i.e. when half the stars have formed). We write the star formation rate in terms of the numerical parameter $\eta \geq 1$ as

$$\dot{M}_* = \frac{M_{*f}}{\eta \bar{t}_{\text{ff}}} = \frac{2M_{*,\text{typ}}}{\eta \bar{t}_{\text{ff}}} = \frac{2M_{\text{cl,typ}}}{3\eta \bar{t}_{\text{ff}}}, \quad (20)$$

where $M_{*,\text{typ}} = 0.5M_{*f}$ is the typical current mass of stars, $M_{\text{cl,typ}}$ is the typical current total mass of the clump, and, for $\epsilon_{\text{core}} = 0.5$, $M_{*,\text{typ}} = M_{\text{cl,typ}}/3$, if the protostellar outflows are efficiently ejected from the clump and most of the clump mass is in cores (see TM02). The star formation rate is then

$$\dot{M}_* = 9.7 \times 10^{-3} \left(\frac{1}{\eta} \right) \left(\frac{M_{\text{cl,typ}}}{1000 M_\odot} \right)^{3/4} \Sigma^{3/4} M_\odot \text{ yr}^{-1} \quad (21)$$

and the cluster formation time is

$$t_{\text{cluster}} = \eta \bar{t}_{\text{ff}} = 6.86 \times 10^4 \eta \left(\frac{M_{\text{cl,typ}}}{1000 M_\odot} \right)^{1/4} \Sigma^{-3/4} \text{ yr}. \quad (22)$$

We wish to estimate the cluster star formation rate, and thus η , from observations. One method is to relate the summed total of many individual stellar

accretion events to the production of a *protocluster wind*, which is the superposition of many individual bipolar protostellar outflows. From equations (19) and (22) the expected momentum injection rate from a forming star cluster is

$$\begin{aligned} \dot{p}_{w,\text{tot}} &= \frac{p_{w,\text{tot}}}{t_{\text{cluster}}} \\ &= \begin{cases} \frac{0.80}{\eta} \left(\frac{\phi_w}{0.5}\right) \left(\frac{M_{\text{cl,typ}}}{10^3 M_\odot}\right)^{0.89} \Sigma^{3/4} M_\odot \text{ km s}^{-1} \text{ yr}^{-1} & \frac{M_{\text{cl,typ}}}{M_\odot} < 1500, \\ \frac{0.85}{\eta} \left(\frac{\phi_w}{0.5}\right) \left(\frac{M_{\text{cl,typ}}}{10^3 M_\odot}\right)^{3/4} \Sigma^{3/4} M_\odot \text{ km s}^{-1} \text{ yr}^{-1} & \frac{M_{\text{cl,typ}}}{M_\odot} > 1500. \end{cases} \end{aligned} \quad (23)$$

We compare equation (23) against observations of outflows from protoclusters (Choi et al. 1993, hereafter C93). The observational determination of $\dot{p}_{w,\text{tot}}$ involves measuring the total outflow momentum over some region and identifying a characteristic timescale of the flow over the scale of this region. The CO observations of C93 cover regions with sizes similar to R_{cl} for which virial mass estimates have been made from CS transitions, tracing dense gas. The spatial extent of the outflow observations is limited by sensitivity and the flows almost certainly continue beyond R_{cl} . This is also evident from the fact that the flow timescales are much shorter than \bar{t}_{ff} . These considerations allow us to neglect the effects of evolution in determining an estimate of the instantaneous star formation rate from the observed flows. Though poorly resolved, the morphologies of the flows appear quasi-spherical, as would be expected if there were multiple driving sources.

From CO line strengths, C93 derive the mass of the flow, correcting for optical depth and excitation temperature effects and assuming standard abundance ratios. The line of sight momentum is then summed over velocity channels. We have further corrected these estimates for projection effects (a factor of two increase for a spherical flow). The total momentum (and mass) of the flow may be greater by the amount contained in atomic gas. For example we have seen in our fiducial model for protostellar winds from an individual core that 62% of the total momentum is in this form (i.e. resides in gas that was processed through the accretion disk). As this flow sweeps up gas beyond the core, the atomic fraction is reduced. TM02 estimate that about 25% of the total momentum is in atomic form, so to recover the total momentum we therefore increase the observed value by 33%. This question may be examined observationally, though current surveys have placed only upper limits on the fraction of atomic momentum in the flows (Choi et al. 1994).

Given estimates of mass and momentum, we determine a characteristic flow velocity, \bar{v}_p , and thus an outflow timescale $t_p = R_p/\bar{v}_p$ (here we use the data uncorrected for projection effects, which should approximately cancel in this ratio). The value of $\dot{p}_{w,\text{tot}}$ is then calculated, and with knowledge of the clump's mass and surface density, used to estimate η . The properties of our sample of protoclusters and their outflows are listed in Tables 1 and 2.

Excluding the cases of Cep A and NGC6334 I(N) (below), we find the logarithmic mean value of η is 10.4. The standard deviation is about a factor of two, consistent with the observational uncertainties. This gives a cluster formation time (eq.[22]) of $7.1 \times 10^5 (M_{\text{cl,typ}}/1000 M_\odot)^{1/4} \Sigma^{-3/4} \text{ yr}$, which is consistent with estimates of $\lesssim 10^6 \text{ yr}$ from the spread in pre-main-sequence ages in the Orion Nebula Cluster (Palla & Stahler 1999), which has $M_{\text{cl}} \sim 4500 M_\odot$ (Hillenbrand

Table 1. Properties of Protoclusters^a

Name	d (kpc)	M_{cl} (M_{\odot})	R (pc)	Σ (g cm^{-2})	L_{bol} ($10^5 L_{\odot}$)
S140(IRS1)	0.9	128	0.14	0.43	0.05
GL490	0.9	91-151	0.06-0.083	1.68-1.44	0.017-0.024
GL2591	1.0	268-320	0.13-0.11	1.05-1.76	0.225
NGC2071	0.39	484	0.69	0.068	0.0052
W3(Main) ^b	2.3	610	0.35	0.33	5.2
Cep A	0.73	787	0.14	2.67	0.17
W28(A2)	2.0	982	0.18	2.0	1.3-1.9
NGC6334 I(N)	1.7	~1700	0.37	0.83	< 0.1

^a Data and lists of primary references for all sources except NGC6334 I(N) (Megeath & Tieftrunk 1999) are in C93, P97, and van der Tak et al. (2000).

^b W3(Main) appears to be a relatively evolved system, containing numerous H II regions, so the virial mass estimates based on observations (P97) of the gas today probably underestimate the initial mass. This can explain why $M_{\text{cl}}/3$ is an insufficient stellar mass to account for L_{bol} .

& Hartmann 1998). We note that the effect of wind-wind interactions, which we have ignored in our analysis, would shorten this estimate by the fraction of wind momentum that is dissipated.

Cep A is the most extreme of the C93 protoclusters in terms of its surface density. The estimates of virial mass and surface density are made uncertain by the fact that 2D maps of the dense gas show moderate elongation (Y. Shirley, private communication). Furthermore, the outflow observations do not symmetrically probe the central region of Cep A (M. Choi, private communication) and so the total $\dot{p}_{w,\text{tot}}$ may be underestimated, thus artificially raising η . For these reasons we have excluded Cep A from our statistical sample. NGC6334 I(N)'s outflow was observed by Megeath & Tieftrunk (1999) and the outflow parameters determined using different techniques to those of C93. This source is thought to be in an extremely early stage of evolution; for example the observed outflow extends over only a small fraction of the clump, which has a relatively low luminosity. Again we exclude this source from the statistical sample, but consider it in the context of an example of the earliest stage of cluster formation.

A common observational diagram used in the study of outflows from protostars and protoclusters plots $\dot{p}_{w,\text{tot}}$ versus L_{bol} . We consider a simple description of the evolution of protoclusters in this diagram. Assuming a constant star formation rate (eq.[21]) implies that, averaged over a population of clusters, $\dot{p}_{w,\text{tot}}$ is a constant over most of the evolution. In the earliest stages the luminosity is small and dominated by that resulting from accretion. The minimum luminosity is $\sim G\bar{m}_*\dot{M}_*/r_*(\bar{m}_*)$, where $\bar{m}_* \lesssim \bar{m}_{*f}$ is the mean protostellar mass. We have $\dot{M}_* = \dot{p}_{w,\text{tot}}/(\phi_w \bar{v}_K)$, where \bar{v}_K is the Keplerian velocity at the stellar surface of an average protostar. The mean radius is about $3 R_{\odot}$ (Figure 1) and thus

$$L_{\text{min}} = 4.3 \times 10^4 \left(\frac{0.5}{\phi_w} \right) \left(\frac{\bar{m}_*}{0.3 M_{\odot}} \frac{3 R_{\odot}}{r_*(\bar{m}_*)} \right)^{1/2} \left(\frac{\dot{p}_{w,\text{tot}}}{M_{\odot} \text{ km s}^{-1} \text{ yr}^{-1}} \right) L_{\odot}. \quad (24)$$

Table 2. Observed Outflows from Protoclusters^a

Name	R_p	t_p	$p_{w,\text{tot}}$	$\dot{p}_{w,\text{tot}}$	η
	HV(EHV) ^b (pc)	HV(EHV) (10 ³ yr)	HV(EHV) (M _⊙ km s ⁻¹)	HV(EHV)[TOT] ^c (10 ⁻³ M _⊙ km s ⁻¹ yr ⁻¹)	
S140(IRS1)	0.20 (0.15)	31 (6.6)	307 (10.2)	10.1 (1.6) [15.4]	4.4
GL490	0.087 (0.087)	9.7 (2.4)	60 (11.8)	6.2 (4.9) [14.8]	9.5-13.2
GL2591	0.097 (0.055)	11.9 (2.4)	131 (3.11)	11.0 (1.3) [16.4]	15.7-27
NGC2071	0.051 (0.044)	4.2 (1.5)	13.2 (3.54)	3.1 (2.4) [7.3]	7.7
W3(Main)	0.39 (0.20)	29 (7.5)	204 (16.2)	7.1 (2.2) [12.2]	18.4
Cep A	0.11 (0.11)	11.3 (3.0)	156 (15.3)	13.8 (5.1) [25.1]	54
W28(A2)	0.14 (0.14)	10 (3.4)	889 (82.7)	88 (24) [149]	8.9
NGC6334 I(N)	0.22 (n/a)	9.5 (n/a)	312 (n/a)	33 (n/a) [44]	25

^a Data from C93, except for NGC6334 I(N) (Megeath & Tieftrunk 1999).

^b C93 outflow data are divided into high (HV) and extremely high (EHV) velocity parts.

^c Includes correction factor of 1.33 for atomic gas (TM02).

Observed protoclusters, selected for showing signs of massive star formation, will tend to be over-luminous compared to equation (24). Those in the earliest stages of evolution should lie systematically closer to the birthline.

The maximum luminosity is approximately the post-accretion luminosity, L_{*f} , for all but the smallest clusters (where accretion can make a significant contribution). We have determined $L_{*f}(M_{*f})$ from Monte Carlo simulations (above). Relating $M_{*f} = 2M_{\text{cl,typ}}/3$ for a typical forming cluster (TM02), we then eliminate $M_{\text{cl,typ}}$ in equation (23). The resulting expression defines the “cluster birthline” (the 3 cases correspond to values of M_{*f}/M_{\odot} of $10^2 - 10^3$, $10^3 - 1.6 \times 10^3$ and $> 1.6 \times 10^3$, respectively):

$$L_{*f} = \begin{cases} 3.5 \times 10^7 \phi_L^{-2.0} \Sigma^{-1.5} \left(\frac{\dot{p}_{w,\text{tot}}}{\text{M}_{\odot} \text{km s}^{-1} \text{yr}^{-1}} \right)^{2.0} L_{\odot} & 6.9 \times 10^3 \lesssim \frac{L_{*f}}{L_{\odot}} \lesssim 4.4 \times 10^5 \\ 7.9 \times 10^7 \phi_L^{-2.4} \Sigma^{-1.8} \left(\frac{\dot{p}_{w,\text{tot}}}{\text{M}_{\odot} \text{km s}^{-1} \text{yr}^{-1}} \right)^{2.4} L_{\odot} & 4.4 \times 10^5 \lesssim \frac{L_{*f}}{L_{\odot}} \lesssim 1.0 \times 10^6 \\ 1.1 \times 10^7 \phi_L^{-4/3} \Sigma^{-1} \left(\frac{\dot{p}_{w,\text{tot}}}{\text{M}_{\odot} \text{km s}^{-1} \text{yr}^{-1}} \right)^{4/3} L_{\odot} & 1.0 \times 10^6 \lesssim \frac{L_{*f}}{L_{\odot}} \end{cases} \quad (25)$$

where $\phi_L = (\phi_w/0.5)(10/\eta)$.

The protocluster and cluster birthlines are shown in Figure 3. In Figure 3a we also plot the results of Monte Carlo simulations of many clusters for two cases: $M_{*f} = 200, 1000 M_{\odot}$. For each cluster, stars are drawn randomly from the IMF and stochastically in time and then followed through our protostellar evolution model for pressures corresponding to $\Sigma = 1 \text{ g cm}^{-2}$. The central/outer lines show the median/68-percentile values of each cluster distribution. Points mark equal time intervals in the evolution. In Figure 3b we plot the observed protoclusters, giving $\dot{p}_{w,\text{tot}}$ a factor of four uncertainty. Sources in an early stage of formation (NGC2071 and NGC6334 I(N)) are close to the protocluster birthline, while those in a late stage (W3(H₂O)—as evidenced by its multiple H II regions) are close to or below the cluster birthline.

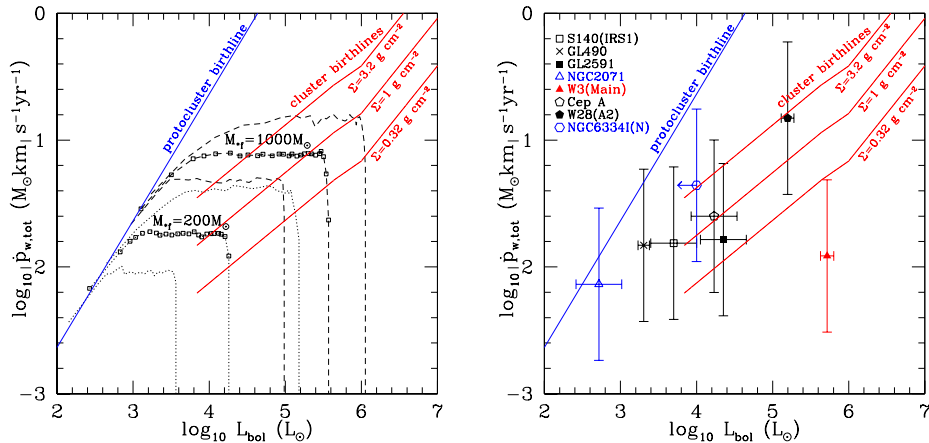


Figure 3. $\dot{p}_{w,\text{tot}}$ versus L_{bol} . (a) Left: Theoretical birthlines and results of Monte Carlo simulations. (b) Right: Observed protoclusters.

5. Conclusions

We have presented a theoretical model for high-mass star formation that determines the accretion rate in terms of the final and instantaneous masses of the star, the ambient pressure surrounding the gas core, and the polytropic index of pressure support. We related the pressure due to self-gravity in the centers of typical Galactic star-forming clumps to their surface density; \bar{P}/k approaches 10^9 K cm^{-3} for typical values of $\Sigma \simeq 1 \text{ g cm}^{-2}$. These pressures allow a $100 M_{\odot}$ star to form in $\sim 10^5 \text{ yr}$ with a final accretion rate $\sim 10^{-3} M_{\odot} \text{ yr}^{-1}$. Modeling protostellar evolution, we predicted the properties of several nearby massive protostars. Under the hypothesis that the outflows from massive protostars are driven magneto-centrifugally in the same manner as those from low-mass protostars, we found that each decade of the IMF contributes approximately equally to the total outflow momentum. This helps to explain the generally poor overall collimation of outflows from high-mass star-forming regions. We utilized these models and observations of outflow intensities from several nearby protoclusters to estimate their star formation rates, finding that these clusters are typically forming over at least several free-fall times. We have proposed theoretical birthlines in the $\dot{p}_{w,\text{tot}}$ versus L_{bol} diagram to delimit the phase of cluster formation.

Acknowledgments. We thank Henrik Beuther, Minho Choi, Neal Evans, Ralph Pudritz, Yancy Shirley, Steve Stahler and Malcolm Walmsley for helpful discussions. Our research is supported by NSF grants AST-9530480 and AST-0098365, by a NASA grant supporting the Center for Star Formation Studies, and (for JCT) by a Spitzer-Cotsen fellowship from Princeton University.

References

- Behrend, R., & Maeder, A. 2001, *A&A*, 373, 190
 Blandford, R. D., & Payne, D. G. 1982, *MNRAS*, 199, 883

- Bonnell, I. A., Bate, M. R., Clarke, C. J., & Pringle, J. E. 1997, MNRAS, 285, 201
- Bonnell, I. A., Bate, M. R., & Zinnecker, H. 1998, MNRAS, 298, 93
- Bontemps, S., Andre, P., Terebey, S., & Cabrit, S. 1996, A&A, 311, 858
- Caselli, P., & Myers, P. C. 1995, ApJ, 446, 665
- Choi, M., Evans, N. J. (II), & Jaffe, D. T. 1993, ApJ, 417, 624 (C93)
- Choi, M., Evans, N. J. (II), Jaffe, D. T., & Walker, C. K. 1994, ApJ, 435, 734
- Hillenbrand, L.A., & Hartmann, L.W. 1998, ApJ, 492, 540
- Jijina, J., & Adams, F. C. 1996, ApJ, 462, 874
- Li, Z.-Y., & Shu, F. H. 1997, ApJ, 475, 237
- Matzner, C. D., & McKee, C. F. 1999, ApJ, 526, L109
- Matzner, C. D., & McKee, C. F. 2000, ApJ, 545, 364
- McKee, C. F., & Tan, J. C. 2002, in preparation (MT02)
- McLaughlin, D. E., & Pudritz, R. E. 1996, ApJ, 469, 194
- McLaughlin, D. E., & Pudritz, R. E. 1997, ApJ, 476, 750 (MP97)
- Megeath, S. T., & Tieftrunk, A. R. 1999, ApJ, 526, L113
- Miller, G. E., & Scalo, J. M. 1979, ApJS, 41, 513
- Najita, J. R., & Shu, F. H. 1994, ApJ, 429, 808
- Nakano, T., Hasegawa, T., Morino, J.-I., & Yamashita, T. 2000, ApJ, 534, 976
- Onishi, T., Mizuno, A., Kawamura, A., Ogawa, H., & Fukui, Y. 1996, ApJ, 465, 815
- Osorio, M., Lizano, S., & D'Alessio, P. 1999, ApJ, 525, 808
- Palla, F., & Stahler, S. W. 1992, ApJ, 392, 667
- Palla, F., & Stahler, S. W. 1999, ApJ, 525, 722
- Plume, R., Jaffe, D. T., Evans, N. J. (II), Martin-Pintado, J., & Gomez-Gonzalez, J. 1997, ApJ, 476, 730 (P97)
- Richer, J., Shepherd, D., Cabrit, S., Bachiller, R., & Churchwell, E. 2000, in *Protostars & Planets IV*, eds. V. Mannings, A. P. Boss, & S. S. Russell (Tucson: The University of Arizona Press), 867
- Salpeter, E. E. 1955, ApJ, 121, 161
- Schaller, G., Schaerer, D., Meynet, G., & Maeder, A. 1992, A&AS, 96, 269
- Shu, F. H. 1977, ApJ, 214, 488
- Shu, F. H., Lizano, S., Ruden, S. P., & Najita, J. 1988, ApJ, 328, L19
- Shu, F. H., Tremaine, S., Adams, F. C., & Ruden, S. 1990, ApJ, 358, 495
- Shu, F. H., Najita, J., Ostriker, E., Wilkin, F., Ruden, S., & Lizano, S. 1994, ApJ, 429, 781
- Solomon, P.M., Rivolo, A.R., Barrett, J., & Yahil, A. 1987, ApJ, 319, 730
- Stahler, S. W. 1988, ApJ, 332, 804
- Stahler, S. W., Shu, F. H., & Taam, R. E. 1980, ApJ, 241, 637
- Tan, J. C., & McKee, C. F. 2002a, in preparation (TM02)
- Tan, J. C., & McKee, C. F. 2002b, in preparation
- van der Tak, F. F. S., van Dishoeck, E. F., Evans, N. J. (II), & Blake, G. A. 2000, ApJ, 537, 283
- Wolfire, M. G., & Cassinelli, J. 1987, ApJ, 319, 850